EGU2016-6478

Automatic Event Bulletin Built by Waveform Cross Correlation using the Global Grid of Master Events with Adjustable Templates

Ivan Kitov, Dmitry Bobrov, and Mikhail Rozhkov
International Data Centre, CTBTO

CTBTO PREPARATORY COMMISSION | preparatory commission for the comprehensive nuclear-test-ban treaty organization

Abstract. We built an automatic seismic event bulletin for the whole globe using waveform cross correlation at array stations of the International Monitoring System (IMS). To detect signals and associate them into robust event hypotheses in an automatic pipeline we created a global grid (GG) of master events with a diversity of waveform templates. For the Comprehensive Nuclear-Test-Ban Treaty (CTBT), the GG provides an almost uniform distribution of monitoring capabilities and adjustable templates. For seismic areas, we select high quality signals at IMS stations from earthquakes. For test sites, signals from UNEs are best templates. Global detection and association with cross correlation technique for research and monitoring purposes demands templates from master events outside the regions of natural seismicity and test sites. We populate aseismic areas with masters having synthetic templates calculated for predefined sets of IMS array stations. We applied various technologies to synthesize most representative signals for cross correlation and tested them using the Reviewed Event Bulletin (REB) issued by the International Data Centre (IDC). At first, we tested these global sets of master events and synthetic templates using IMS seismic data for February 13, 2013 and demonstrated excellent detection and location capability. Then, using the REB and cross correlation bulletins (XSELs) experienced analysts from the IDC compared the relative performance of various templates and built reliable sets of events and detections for machine learning. In this study, we carefully compile global training sets for machine learning in order to establish statistical decision lines between reliable and unreliable event hypotheses, then apply classification procedures to the intermediate automatic cross correlation bulletin based on the GG, and compile the final XSEL, which is more accurate and has lower detection threshold than the REB.

Conclusion. This work extends the research we presented at the Science and Technology 2015 conference regarding the construction of Global Grid of master events for seismic monitoring with waveform cross correlation.

Using the catalogue of seismic events (REB) created by the IDC, we have done some preliminary estimates of the portion of valid events obtained by waveform cross correlation. Machine learning was a natural choice for selection of valid events from the extremely large amount of data. As in other areas, we doubled the number of events in the REB, with all new events matching the IDC event definition criteria.

We have created a prototype of cross-correlation-based Global Grid monitoring system, which has been tested at the IDC during the past years and for this study was populated with one synthetic template obtained by the PCA (Principal Component Analysis) of real waveforms from a hundred of underground nuclear tests distributed over the world. One template waveform was replicated over all stations and individual channels. Time delays between individual channels of an array were calculated for master event-station theoretical slownesses.

To use machine learning at the global level it is necessary to create a training dataset populated with valid events created by waveform cross correlation as well as false events created by the same method. Here we use the REB to build a cross correlation event list and process only data at relevant stations. To reduced calculations, we have processed only time intervals around known REB events. Two days, February 13 and 14, were processed continuously and a large number of false events together with associated detections were build.

Overall, we have demonstrated a significant increase in the number of detected arrivals when cross correlation is used. The obtained events and arrivals were used for training of various classification algorithms applied in the framework of continuous processing with cross correlation.

The Global CC Grid technique gives an opportunity for complete implementation of CC-based global detection and location. The specific features of the P-waves from underground nuclear tests used in this study can reduce the global detection threshold of seismic monitoring under the CTBT by 0.4 to 0.5 units of magnitude. This corresponds to the reduction in the test yield by a factor of 2 to 3 for any location and depth of burial. Considering the history of seismic monitoring of UNEs this is a crucial improvement which can be also enhanced by a more effective use of IMS array stations.

SEISMIC MONITORING: EXPLOSIONS CAN BE CONDUCTED ANYWHERE

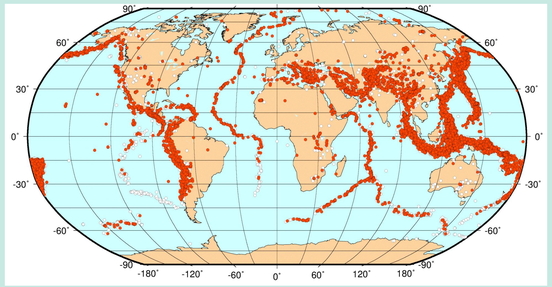

Figure 1. Map of REB events found during 2013. Red circles – events found by cross correlation (i.e. two or more REB phases are within 4 s). White circles – not found events –most included 3-C stations not considered for waveform cross correlation at this stage.

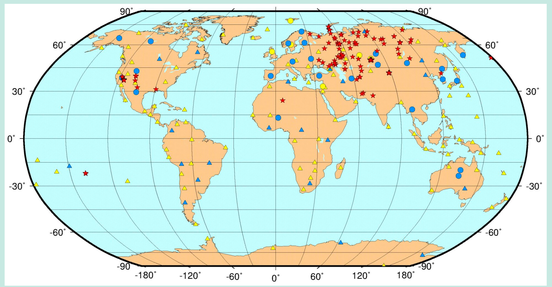

Figure 2. A map of IMS seismic network with historical UNEs. Blue circles – primary arrays, blue triangles – primary 3-C stations. Yellow circles – auxiliary arrays, yellow triangles – auxiliary 3-C stations. Red starts – underground nuclear explosions. Only primary arrays are used for cross correlation.

An underground nuclear test can be conducted in any place on the planet, not only in seismic regions. Figure 1 presents a map of events from the Reviewed Event Bulletin (REB) as found by the International Data Centre (IDC) in 2013. Figure 2 shows the Seismic Network of the International Monitoring System (IMS) and relative positions of selected historical underground nuclear tests. The difference between geographical distribution of earthquakes and explosions is striking.

The technique of waveform cross correlation (matched filter) is naturally based on high-quality waveform templates from a representative set of master events. In seismic areas, one can use waveform templates from natural events. Similarly, one can use signals from underground nuclear tests where available. And for the rest of the world we need the best possible templates for the purpose of seismic monitoring. Here we present and test the performance of the uniformly distributed Global Grid (GG) of master events designed for the best performance of waveform cross correlation.

The events in the REB with detections found by cross correlation at two and more IMS arrays are then used to build training sets for machine learning. The events built by cross correlation and not found in the REB are also used for training as noise.

Figure 3 presents the global coverage by master events. A small segment of the GG is shown in Figure 4. Each node contains a master event with templates at IMS array stations. Since the IMS network is sparse, the number of stations associated with a given master may vary from 3 to 10. The quality, sensitivity, and resolution of an array depend on many factors; its aperture and number of sensors are likely among the most important.

Considering the design and historical performance of the primary IMS arrays we have to distribute them over three quality groups. For a given master, we use arrays from Group 2 and 3 only when no array from Group 1 is available. The largest number of IMS stations associated with a master is 10. The smallest number is 3 as dictated by the strict IDC requirement for a valid REB event. There are some areas where 3 primary arrays are not available. Currently, we are extending the set of stations to use templates from 3-C stations to build master events for nodes in the not covered areas.

Each node or master event is responsible for a circular footprint of ~125 km in radius. The distance between nodes is approximately 140 km. Therefore, the GG covers the whole earth without any blind areas. It is important that the zones of responsibility of neighboring nodes intersect. Figure 5 presents the detailed design of the nodes. For all (~23,500) nodes, cross correlation with templates at each associated station is calculated.

WAVEFORM TEMPLATES, CROSS CORRELATION, EVENT BUILDING

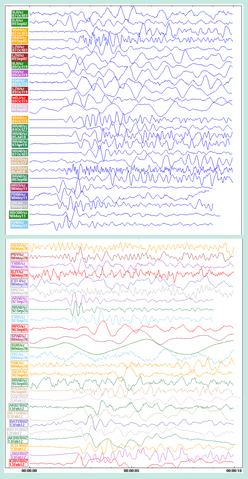

Figure 6. Real seismograms with varying distance, depth, and UNE source functions which were used in PCA.

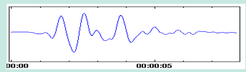

Figure 7. The PCA 1st component is used as a universal template for all stations and channels

Despite its original design aimed at seismic monitoring of nuclear tests, waveform templates for the GG can be selected from a broader set of signals depending on the nature of target seismic sources. Here, we follow the way known as a signal dimensionality reduction.

The dimensionality reduction allows finding a template best describing the set of records of nuclear explosions conducted in wide ranges of epicentral distance, rock types, yield, and depth of burial. Some examples of such waveforms are presented in Figure 6. These real seismograms have different sampling rate and were recorded by sensors with different responses. Therefore, they were all reduced to one sensor type and sampling rate.

Principal Component Analysis (PCA) performed with Singular Value Decomposition (SVD) is used as a tool to build templates. Figure 7 demonstrates the first principal component obtained by the PCA. This waveform was used to build synthetic templates for all channels and all arrays. The only difference between the templates was in the sampling rate which varies from 20 Hz to 80 Hz for IMS array stations. For a given array, time delays between channels were calculated from theoretical travel time curves according to master/station positions.

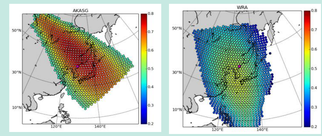

Figure 8. For a set of master events around the DPRK-2013, sample distributions of cross correlation coefficient between master templates and real waveforms from the 2013 DPRK for array stations AKASG and WRA. Almost all masters have detections at AKASG and WRA. These detections and detections at other 8 IMS stations are used to build event hypotheses.

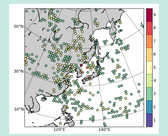

Figure 9. Finding the 2013 DPRK with the Global Grid. The number of stations associated with the event hypotheses obtained in local association process. Only the hypotheses with 3 and more associated stations are shown. The best hypothesis has 9 associated stations and is the closest to the test position estimated from satellite data. All detections at the involved array stations are found using the first PCA component shown un Figure 7.

USING THE REB FOR TESTING GG PROCEDURES

In order to assess the portion of correct hypotheses which can be potentially built by the GG we have tested a smaller case of seismicity in North Atlantic region. Because of task dimension, machine learning was used with the MATLAB TreeBagger tool as the first choice. Following general procedure for this application, we have compiled a dataset containing two classes of arrivals as associated with valid and invalid (strictly according to the IDC definition) events. To populate the set of valid events and detections, we selected the event hypotheses obtained by the GG, which have close origin times to the events reported in the REB.

Overall, we selected 258 valid event hypotheses obtained by the GG prototype for the training set. The set of invalid events was created by a random choice of ~3% (1859) of the hypotheses far enough (600 s) from the REB events. In total, the class of valid events included 1031 arrivals at 7 IMS array stations and there were 5631 arrivals associated with the events not matching REB criteria.

After training, we classified 177,520 arrivals in 48,443 hypotheses. Classification algorithm allowed to build 252 new valid events defined by three or more valid arrivals as required by the IDC event definition criteria. Figure 10 displays locations for these qualified events, which repeat the pattern of the Mid-Atlantic Ridge seismicity.

To be included in the REB, all selected hypotheses have to be confirmed interactively. As in our previous studies, cross correlation approximately doubles the amount of REB events and reduces the detection threshold by 0.4 magnitude units.

Figure 10. Locations of 252 new qualified event hypotheses, which match the REB criteria.

GLOBAL CROSS CORRELATION GRID: DESIGN

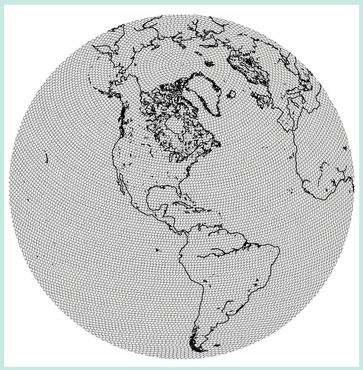

Figure 3. Global Grid for Cross Correlation. There are ~23,500 nodes in the GG. Each node represent a master event with 3 to 10 waveform templates at primary IMS array stations.

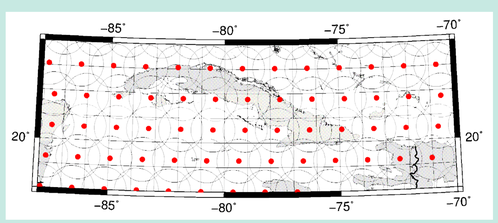

Figure 4. Sample segment of the Global Grid.
- Spacing between grid points (masters) ~140 km.
- P-wave templates from three to ten IMS primary arrays per master
- Distance for P (Pn)-phase from 6 to 96 degrees
- At least three IMS stations to create an REB event

Feasible templates:

- Real waveforms from events near the GG nodes,
- Grand masters – best events replicated over larger sets of GG nodes
- Synthetic waveforms - any source function, mechanism, depth, location, etc.

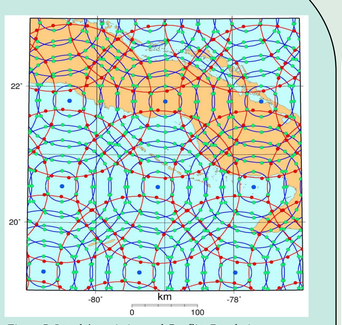

Figure 5. Local Association and Conflict Resolution
1. Five circles with ~25 km increment in radius.
2. 91 nodes for origin time calculation (green points)
3. All hypotheses at the outer circle (red points) are rejected since they have to be created by neighbouring masters.

Global Grid design, 23,500 nodes

Array stations arranged by quality:
Group 1 = WRA, TORD, MKAR, ILAR, GERES, PDAR, CMAR, SONM, AKASG, BRTR, GEYT
Group 2 = ASAR, ZALV, YKA, ARCES, TXAR, KSRS
Group 3 = USRK, FINES, NVAR, NOA, MJAR

GCCG quality criteria:
XSEL event: NSTAmin = 3; dTorigin = 6s; AZGAPmax = 330º
Detections: SNRmin = 0.5; SNR_CCmin = 2.5; |CCmin | = 0.2;
Quality check: FKSTATmin = 2.5; AZRESmax = 20.0º; SLORESmax = 2.0 s/º

Relevant signals are detected by STA/LTA technique applied to the trace of cross correlation coefficient averaged over all channels without time shifts – for two events close in space cross correlation peaks simultaneously at all channels. All detected signals have to match a number of quality criteria as obtained by statistical and FK-analysis. For all detections, their arrival times are projected back to master events by theoretical travel times.

Using the full set of origin times for a given master, we build slave event hypotheses. In order to better predict the origin times, each node has five circles of hypothetical locations for the sought (slave) events where travel times to the stations relevant for the given master event are predicted (Figure 5); the spacing between circles is 25 km and the outer circle has radius of 125 km. Because the outer circle (red points) of a given master intersects with internal circles of the neighboring masters we reject all final event hypotheses built on this outer circle. Such hypotheses must belong to the neighboring events. Other conflicts between event hypotheses belonging to neighboring events are resolved by the number of stations and the standard deviation of origin times for arrivals on the associated stations.

MACHINE LEARNING FOR THE GCCG

The current study includes three stages. At first, we conducted cross correlation of the templates based on the first PCA component in Figure 7 with the waveforms likely containing signals from all seismic events included in the 2013 REB. The set of successful detections of the REB events (2 and more arrivals for one event) builds a part of training set. Secondly, we built complete cross correlation bulletins (XSELs) for February 13 and 14, 2013. Finally, we applied various machine learning methods to the training set containing valid detections (i.e. in the XSEL events matched in the REB) and false detections (i.e. those in the XSEL events not matched in the REB) and classified all events hypotheses in the XSELs for Feb. 13 and 14. The resulting XSEL is considered as a substitute to the REB.

From 33,710 REB events built in 2013, we used 30,513, which have 2 and more primary IMS arrays. Only master events within 1400 km from the REB events were used to populate the set of valid events. Time windows included the segment -5 min to +5 min from the expected arrival times on stations related to each master. The reduced set of masters (around 300 instead of ~25,000 in the GG) and short time window allow fast calculation for one year.

All cross correlation detections for all masters were used to build event hypotheses and, after local association and conflict resolution, the best events are saved in an XSEL. At this stage, the principal goal is to find more arrivals at IMS array stations than listed in the REB for future use in machine learning. We define an REB arrival as found when there is a cross correlation detection within 4 s.

There are 16,318 REB events having 2 and more arrivals found by cross correlation. At the same time, we find many arrivals at other stations of the same master, which were not detected by standard procedures. Figure 11 shows the numbers of found REB detections and added detections for 22 stations.

For a synthetic template, theoretical time delays between channels and the absence of empirical SASCs may lead to poor azimuth and slowness estimates as obtained by the FK-analysis of cross correlation traces. Before building event hypotheses, we used the closest masters to detect signals near those existing or expected in the REB. The number of found and added arrivals has increased. Figure 12 demonstrates that there are many more detections with slowness and azimuth residuals beyond the predefined limits.

The best stations like WRA have very low proportion of such detections as they provide reliable estimates of the studied parameters. However, judging by the distribution of CC and SNR_CC for these detections many of them are of relatively high quality and thus can be use in local association and then in .

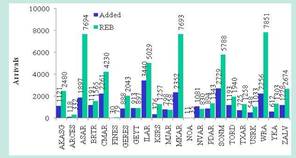

Figure 11. The number of found REB and added detections. Most effective stations (WRA,ASAR,MKAR …) have relatively low proportion of added events. Poor stations may add as many arrivals as found in the REB.

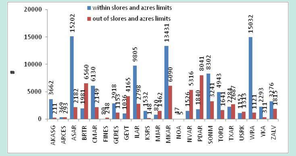

Figure 12. The number of arrivals found by CC within the predefined Azres and Slowres limits and added detections out of these limits. Most effective stations WRA, ASAR, MKAR … have very low proportions of added arrivals.

To perform machine learning with valid and false detections we used **scikit-learn** (0.17.1, www.scikit-learn.org) - a set of python modules for machine learning and data mining. In order to optimize machine learning for monitoring purposes, we have tested various applications including**:** SVM with linear kernel, SVM with *Radial Basis Function* kernel, Decision Tree, Nearest Neighbors, Random Forest, AdaBoost, Naive Bayes, Linear Discriminant Analysis, and Quadratic Discriminant Analysis. Cross-validation tests were carried out 3 times - 2/3 for learning and 1/3 for test. To assess the output we used **Precision,** i.e. the proportion of instances predicted as positives that were correctly evaluated, **Recall**, i.e. the proportion of positive instances that were correctly evaluated, and **F1-score**, the harmonic mean of precision and recall. The harmonic mean is used instead of the arithmetic mean because the latter compensates low values for precision and with high values for recall. On the other hand, with harmonic mean we will always have low values if either precision or recall is low.

After a thorough investigation we have selected **Random Forest** algorithm which uses perturb-and-combine techniques specifically designed for trees. This means a diverse set of classifiers is created by introducing randomness in the classifier construction. The prediction of the ensemble is given as the averaged prediction of the individual classifiers. Station results are shown in the table.

STA	#	Class	Precision	Recall	F1
AKASG	1202	S	0.993	0.998	0.995
AKASG	18	N	0.832	0.490	0.611
ARCES	150	S	0.987	0.993	0.990
ARCES	6	N	0.794	0.667	0.708
ASAR	3210	S	0.976	0.987	0.982
ASAR	226	N	0.878	0.654	0.712
BRTR	920	S	0.972	0.963	0.967
BRTR	546	N	0.938	0.954	0.946
CMAR	2166	S	0.984	0.989	0.987
CMAR	169	N	0.855	0.796	0.824
FINES	37	S	0.963	0.993	0.978
FINES	6	N	0.752	0.733	0.737
GERES	978	S	0.995	0.997	0.996
GERES	44	N	0.937	0.885	0.909
GEYT	604	S	0.960	0.934	0.947
GEYT	299	N	0.874	0.922	0.897
ILAR	2831	S	0.966	0.964	0.965
ILAR	722	N	0.861	0.868	0.864
KSRS	545	S	0.990	0.995	0.993
KSRS	25	N	0.883	0.780	0.824
MJAR	520	S	0.964	0.964	0.964
MJAR	76	N	0.753	0.750	0.752
MKAR	3356	S	0.974	0.980	0.977
MKAR	517	N	0.863	0.828	0.845
NVAR	639	S	0.951	0.960	0.956
NVAR	174	N	0.850	0.818	0.833
PDAR	747	S	0.960	0.943	0.951
PDAR	424	N	0.903	0.930	0.916
SONM	2847	S	0.976	0.977	0.976
SONM	436	N	0.847	0.841	0.844
TORD	1046	S	0.974	0.970	0.972
TORD	404	N	0.923	0.932	0.927
TXAR	663	S	0.951	0.947	0.949
TXAR	171	N	0.906	0.913	0.909
USRK	529	S	0.978	0.980	0.979
USRK	47	N	0.769	0.752	0.760
WRA	3380	S	0.980	0.990	0.985
WRA	203	N	0.804	0.664	0.727
YKA	642	S	0.977	0.971	0.974
YKA	272	N	0.934	0.945	0.939
ZALV	1304	S	0.971	0.969	0.970
ZALV	224	N	0.821	0.833	0.827

We have tested two sets of parameters used for signal classification. First set included only parameters which were associated with detections: CC, SNR_{CC}, SNR, residuals of azimuth and slowness, etc. In the second set, we also used the number of arrivals associated with a given valid or false event, the averaged and cumulative CC for this event.

For the first set, the XSEL includes 166 REB-compatible events from the total of 285 in the official REB. In this XSEL, there were 153 events having 3 and more arrivals within 4 s from the arrivals in one REB event, and 159 events with 2 and more found REB arrivals. Essentially, the XSEL based only on detection parameters can find only REB events.

The second set of parameters produced 10,145 XSEL events and, after application of the classification based on the results of Random Forest training, the final XSEL included 349 REB-compatible events. In this XSEL, 86 events had 3+ arrivals in the REB, and 143 events 2+ arrivals.

In order to achieve higher performance and XSEL reliability we have to merge both approaches.

Preparatory Commission for the Comprehensive Nuclear-Test Ban Treaty Organization,
Provisional Technical Secretariat, Vienna International Centre, P.O. Box 1200, A-1400
Vienna, Austria. E-mail: ivan.kitov@ctbto.org

www.ctbto.org